



The study of combustion and heat transfer performance of porous combustor-heater with in-bed heat extraction

Prinya Pookertsin and Sumrerng Jugjai *

Department of Mechanical Engineering, King Mongkut's University of Technology Thonburi (KMUTT),
Bangkok, Thailand 10140

* Corresponding Author: Tel: (662) 470 9128, Fax: (662) 4709111,

E-mail: sumrueng.jug@kmutt.ac.th

Abstract

Porous combustor-heater (PCH) with in-bed heat extraction is a combined combustion and heat transfer device in which heat transfer surfaces are embedded directly within packed bed of porous medium wherein premixed gaseous fuel is burned. During past decade, the PCH has received more attention by many researchers. However, none of the literature works illustrates flame zone and thermal structure by a direct measurement of temperature along the PCH axis, and discloses the complex heat transfer phenomena of the PCH. In order to broaden the knowledge, this work conducts an experimental study on 21 kW PCH with three rows of staggered tube bank to clarify the thermal structure, heat transfer performance and emission characteristic. In addition, the simplify calculation method is presented to reveal the heat transfer contributions (conduction, convection and radiation) to the tube bank with the purpose of exploring the complex heat transfer phenomena of the PCH. The results show that flame zone can be located and stabilized within the tube bank yielding highest heat transfer rate of 274 kW/m^2 with extremely low CO and NO_x emission (i.e. 14 ppm and 24 ppm, respectively) at optimum operating equivalence ratio of 0.64. Furthermore, the study of heat transfer contributions reveals that both convection and radiation play an important role for transferring combustion heat to the tube bank. Radiative contribution is enhanced when operated at rich condition (up to 58% of the total rate). In contrast, convective contribution is enhanced when operated at lean condition (up to 50% of the total rate). As expected, conduction, which results only about 10% of total rate, is not significant contribution for enhancing heat transfer to the tube bank.

Keywords: combustion, porous medium, premixed gaseous fuel, combustor-heater, in-bed heat extraction, heat transfer contributions.

Table. 1 Nomenclature

| Symbols | | Subscripts | | Greek Symbols | |
|-----------|--|------------|--|---------------|---|
| A | heat transfer area of the tube (m^2) | $calc$ | calculated from simplify method | σ | Stephan-Boltzmann constant |
| B | $=1.25 \cdot [(1-\phi)/\phi]^{10.9}$ | $cond$ | conduction | | $= 5.67 \times 10^{-8} (W/m^2 \cdot K^4)$ |
| CL | heat supply or firing rate (kW) | $conv$ | convection | ε | radiative emissivity (-) |
| C_p | specific heat (J/kg-K) | exp | calculated from the experiment | μ | Dynamics viscosity (Pa-s) |
| D | tube diameter (m) | f | flame | ϕ | porosity (-) |
| h | heat transfer coefficient ($W/m^2 \cdot K$) | g | gas phase | λ | $= k_g / k_s$ |
| k | thermal conductivity ($W/m \cdot K$) | i | number of tube = 1, 2, ..., 8 | | |
| L | tube length (m) | in | in flow (for T or \dot{m}) or inner (for D) | | |
| \dot{m} | mass flow rate (kg/s) | j | row order = 1, 2, 3 | | |
| n | number of tube in considered row | out | out flow (for T or \dot{m}) or outer (for D) | | |
| Q | heat transfer rate (kW) | rad | radiation | | |
| \bar{Q} | heat transfer rate per total area (kW/m^2) | s | solid phase | | |
| S | conduction shape factor | tb | tube bank | | |
| T | temperature ($^{\circ}C$) | w | water | | |

1. Introduction

Recently, due to public concern in energy utilization with low pollutant emission, a porous medium combustion technology has received more attention. Several works have been devoted on enhancing the radiation efficiency, extending of flammability limit, and fuel reforming [1]. Only little attention has been focused on a porous combustor with in-bed heat extraction. This application is called a porous combustor-heater (PCH), which is a combustion heat transfer device involving relatively cold heat exchange surfaces (or tubes) embedded directly in the porous medium in which gaseous fuel is burned. Xiong et al. [2] conducted an experimental study on the PCH, which consists of tube bank embedded in porous medium as thermal load. Their results demonstrated that flame location is found to be an important variable that strongly affected both heat transfer and combustion performance. It was suggested that the flame should be located outside, and closely to the tube bank in order to achieve a desirable high heat transfer rate. However, the movement flame was studied by observing flue

gas temperature and rate of heat transfer to the tube bank rather than by a direct measurement of temperature distribution along the PCH axis. Shi et al. [3] conducted a numerical modeled base on the experiment of [2]. Most of their numerical results compare reasonably well with the experimental data except for the flame location. Experimental results observed the flame movement though the tube bank, wherein the predictions reveal only stationary flame located outside the tube bank.

The PCH provides several advantages compared to the conventional heat exchanger. However, its development is not far advanced because the complex heat transfer phenomena of PCH have not hitherto been fully understood. In order to broaden the knowledge, this work will conduct the experiment on the PCH whereas the movement of flame can be observed by measuring temperature profiles along the PCH axis directly. In addition, simplify calculation method is presented for revealing the heat transfer contributions (conduction, convection and radiation) to the tube bank with the

challenge of exploring the complex heat transfer phenomena of the PCH.

cooled flame traps, which its design similar to [4], are also embedded in the terminal sections of the test unit to prevent flash back. The water

Table 2 Operating conditions

| Quantity | value |
|---|-------------------------|
| Alumina pellets diameter, d_p | 16×10^{-3} m |
| Equivalence ratio, ϕ | 0.61-0.83 |
| Firing rate, CL | 21 kW |
| Inlet temperature of gas, $T_{g,in}$ | 303 K |
| Inlet temperature of water, $T_{w,in}$ | 303 K |
| Inside surface area per one tube, $A_i = \pi D_{in} L$ | 0.0040 m ² |
| Longitudinal tube pitch, S_L | 47.3×10^{-3} m |
| Number of tubes of tube bank | 8 |
| Outside surface area per one tube, $A_o = \pi D_{out} L$ | 0.0061 m ² |
| Porosity, ϕ | 0.42 |
| Total water mass flow rate at tube bank, $\dot{m}_{w,tb}$ | 7.44 kg/min |
| Total heat transfer surface area, $A_b = 8 \cdot A_o$ | 0.049 m ² |
| Transverse tube pitch, S_T | 50×10^{-3} m |
| Tube inside diameter, D_{in} | 9×10^{-3} m |
| Tube outside diameter, D_{out} | 13.5×10^{-3} m |
| Water tube thermal conductivity, k_{ss} | 13.4 W/m-K |

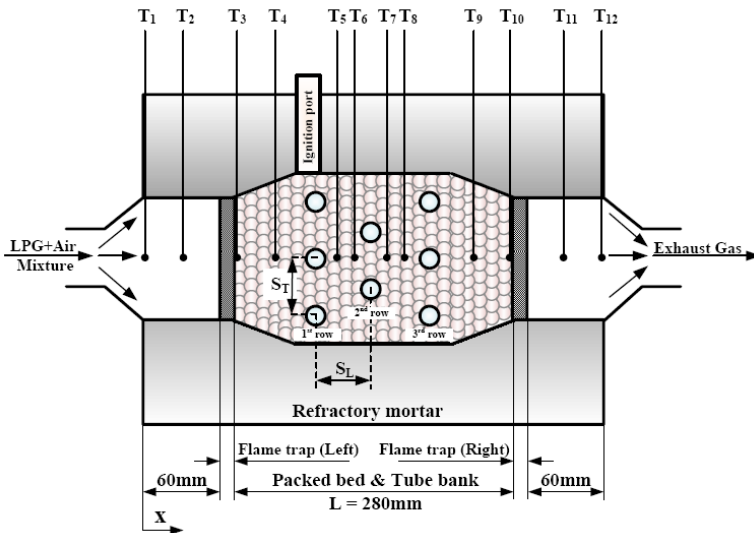


Fig. 1 Porous combustor-heater (test section)

2. Experiment Apparatus

The experimental test section of the PCH is shown schematically in Fig. 1. The combustor has 143×145 mm² configuration and insulating with refractory mortar. Premixed gas of air and liquefied petroleum gas (LPG) is supplied to the combustor by a calibrated rotameters. Three rows of staggered water tube bank is embedded within a packed bed of spherical alumina pellets at the center of the PCH served as in-bed heat exchanger unit to remove combustion heat. Row order of the tube bank is counted along with flow direction. The pitch distance of tube arrangement is chosen to be 1.7 and 1.6 times higher than that of using in the previous work of Jugjai and Nunngiyom [4] for transverse and longitudinal tube pitch, respectively, which is preliminary investigated to be the suitable pitch expansion for relaxation of quenching effect allowing flame movement toward the tube bank. Moreover, two water-

flow rate for each tube ($\dot{m}_{w,tb,i}$) can be independently adjusted and measured by calibrated flow meters. However, an equal flow for each tube was used throughout the experiment with total flow rate ($\dot{m}_{w,tb}$) of 7.44 kg/min.

Temperature measurement in the PCH comprising the temperature ($T_1 - T_{12}$) in Fig. 1 are performed with two types of thermocouples depending on location. Within the packed bed, six B-type thermocouples ($T_4 - T_9$) are used. At both terminal locations ($T_1 - T_3$ and $T_{10} - T_{12}$) are performed with N-type thermocouples. It must be noted that all temperatures measured within the packed bed represent the solid phase temperature. In addition, the inlet and outlet water temperature ($T_{w,in}, T_{w,out,i}$) of each tube are measured by K-type thermocouples. Their signals are digitized by a general-purpose DT 605 Data logger, and then are transmitted to a personal computer. Moreover, emission analysis

of dry combustion product at the exit of the test section is carried out by using the Messtechnik Eheim model Visit01L. All measured emissions are corrected to 0% excess air.

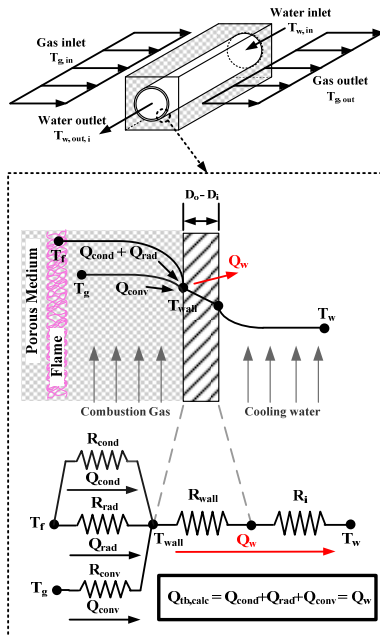


Fig. 2 Simplify thermal resistance model of the PCH (show only one tube)

3. Procedure

Combustion is started by ignition of an auxiliary pilot flame through an ignition port. During the ignition, only the flame traps are supplied by cooling water with total mass flow rate of 9.35 kg/min to control the boundary condition at both terminals, whereas the tube bank are not. Then, premixed gases with equivalence ratio (ϕ) close to one are supplied into the combustor at initial firing rate (CL) of 6.5 kW. Once ignition is accomplished, the auxiliary flame is removed, and CL , ϕ and $\dot{m}_{w,tb}$ gradually adjusted to obtain the desired operating condition. All numerical values of operating conditions appearing in the experiment are summarized in Table. 2.

4. Data reduction

In this present study, the heat transfer performance of the PCH is evaluated by the experimented total heat transfer rate ($Q_{tb,exp}$) to the tube bank, which can be written as

$$Q_{tb,exp} = \sum_{i=1}^8 [\dot{m}_{w,i} \cdot C_{p,w} \cdot (T_{w,out,i} - T_{w,in})] \quad (1)$$

Moreover, the heat transfer performance of PCH can also be evaluated by the calculated total heat transfer rate ($Q_{tb,calc}$), which is defined as a combination of conduction, convection, and radiation contribution to the tube bank:

$$Q_{tb,calc} = Q_{cond} + Q_{conv} + Q_{rad} \quad (2)$$

In order to find those contributions, in this following section, we will discuss about the simplify calculation method for calculating the heat transfer contribution with the purpose of exploring complex heat transfer phenomena of the PCH. The measured temperature profiles along the PCH axis and both inlet and outlet water temperature will be used in the calculation. But first some general assumption must be made to simplify the complexity of the PCH configuration:

1. Heat transfer to the tube bank is considered as one dimensional steady flow process.
2. The measured temperature is considered to be uniform along the cross section of the PCH. Therefore, for each row, the tubes are in the same boundary condition and temperature gradient. Hence, for each row of tubes, the water tube wall temperature is assumed to be constant.

3. Air is assumed to be working fluid instead of exhaust gas with negligible in gas phase radiation.
4. Gas and solid are in thermal equilibrium, so the measured solid temperature can be used as gas temperature for calculated the convective contribution.
5. Solid radiation is equivalent as conduction. Therefore, radiative thermal conductivity of porous medium will be used in the calculation for radiative contribution.

According to the assumptions, the thermal resistance of the PCH can be simplified as illustrated in Fig. 2. It must be noted that heat transfer to the tube will be calculated row by row and then summarized to the total rate.

As illustrated in Fig. 2, both conduction and radiation heat is transferred by the driving force temperature different of flame temperature (T_f), which is indicated by the maximum measured temperature of the PCH, and water tube wall temperature (T_{wall}). Therefore, the conduction contribution can be simplified as

$$Q_{cond} = \sum_{j=1}^3 [Q_{cond,j}] = \sum_{j=1}^3 [n_j \cdot k_{cond} \cdot S_j \cdot (T_f - T_{wall,j})] \quad (3)$$

where T_f is the maximum temperature measured from the experimental, S is the conduction shape factor for embedded circular tube [5], k_{cond} is an effective thermal conductivity of packed bed, and n is number of tube in the considered row. Moreover, the subscript j denotes the order of considered row.

In the same manner, the radiation contribution can also be simplified as

$$Q_{rad} = \sum_{j=1}^3 [Q_{rad,j}] = \sum_{j=1}^3 [n_j \cdot k_{rad} \cdot S_j \cdot (T_f - T_{wall,j})] \quad (4)$$

where k_{rad} is the radiative thermal conductivity of packed bed. Furthermore, the effective thermal conductivity including radiation of packed bed can be expressed [6]:

$$k_{eff} = k_{rad} + k_{cond} \quad (5)$$

where k_{eff} is the sum of conductivity due to conduction and radiation, and can be expressed, respectively, as

$$k_{cond} = 0.8 \times k_g \left\{ 1 - \sqrt{1 - \phi} + \frac{2\sqrt{1 - \phi}}{1 - \lambda B} \right. \\ \left. \times \left[\frac{(1 - \lambda)B}{(1 - \lambda B)^2} \ln\left(\frac{1}{\lambda B}\right) - \frac{B + 1}{2} - \frac{B - 1}{1 - \lambda B} \right] \right\} \quad (6)$$

$$k_{rad} = 4 \cdot \varepsilon \cdot d_p \cdot \sigma \cdot \bar{T}^3 \quad (7)$$

where \bar{T} is average temperature along the heat exchanger section of the PCH (from T_4 to T_9).

In addition, as illustrated in Fig. 3, the temperature difference for convection heat is considered as log-mean temperature difference between inlet and outlet gas phase temperature ($T_{g,in,j}$, $T_{g,out,j}$) and wall temperature. Therefore, the convective contribution can be simplified as

$$Q_{conv} = \sum_{j=1}^3 [Q_{conv,j}] \quad (8)$$

$$= \sum_{j=1}^3 \left[n_j \cdot h_{o,j} \cdot A_{out} \cdot \frac{(T_{g,out,j} - T_{wall,j}) - (T_{g,in,j} - T_{wall,j})}{\ln\left(\frac{T_{g,in,j} - T_{wall,j}}{T_{g,out,j} - T_{wall,j}}\right)} \right]$$

where h_o is convective heat transfer coefficient for flow past embedded staggered tube bank within porous medium. It is appropriate to stated that the correlation for h_o involving with the same configuration of the PCH is hardly found in literature. Heretofore, only the work of Mohammad [7], which numerically investigates

the convective heat transfer of flow past staggered tube bank embedded in porous medium, seems to be the most similar configuration to the PCH. The following correlation is purposed based on the graphical information of [7] with less than 10% of discrepancy:

for first row

$$h_{o,j=1} = \left(1.50 \cdot Re_{max}^{0.521} \cdot \left(\frac{k_s}{k_g} \right)^{0.339} \right) \cdot \frac{k_g}{D_{out}} \quad (9)$$

for second and third row

$$h_{o,j=2,3} = \left(4.67 \cdot Re_{max}^{0.424} \cdot \left(\frac{k_s}{k_g} \right)^{0.483} \right) \cdot \frac{k_g}{D_{out}} \quad (10)$$

where Re_{max} is maximum Reynolds number at minimum free flow area of tube bank, which can be expressed in the term of inlet mass flow rate of gaseous mixture ($\dot{m}_{g,in}$) as

$$Re_{max} = \frac{4 \cdot \left(\frac{S_T}{S_T - D_{out}} \right) \cdot \dot{m}_{g,in}}{\mu_g \cdot \pi \cdot D_{out}} \quad (11)$$

In addition, the gas phase temperature ($T_{g,out,j}$ and $T_{g,in,j}$) in Eq. (8) is obtained from the measured temperature profile along the PCH axis in the experiment. Therefore, T_5 , T_7 , and T_9 can be represented as $T_{g,out}$ for first, second and third row, respectively. Also, T_4 , T_6 , and T_8 can be represented as $T_{g,in}$ for first, second and third row, respectively.

According to Fig. 2, combined heat transfer rate ($Q_{cond} + Q_{conv} + Q_{rad}$) is transferred pass through wall to the water flow inside tube. Therefore, consider heat balance at water tube wall, heat transfer to water-side for each row can be simplified as

$$Q_{cond,j} + Q_{conv,j} + Q_{rad,j} = Q_{w,j} \quad (12)$$

where Q_w is water-side heat transfer rate, which can be express as

$$Q_{w,j} = n_j \cdot \left(\frac{\left(\frac{T_{wall,j} - T_{w,out,j}}{T_{wall,j} - T_{w,in}} \right) - \ln\left(\frac{T_{wall,j} - T_{w,out,j}}{T_{wall,j} - T_{w,in}} \right)}{\frac{\ln(D_{out}/D_{in})}{2 \cdot \pi \cdot k_{SS} \cdot L} + \frac{1}{h_w \cdot A_{in}}} \right) \quad (13)$$

where h_w is water-side heat transfer coefficient calculated from Gnielinski correlation [5], and $T_{w,out,j}$ is bulk mean average water outlet temperature of considered row.

Consequently, for each considered row, Eq. (12) can be expressed as

$$\left(\begin{aligned} & \left[n_j \cdot k_{cond} \cdot S_j \cdot (T_f - T_{wall,j}) \right] + \\ & \left[n_j \cdot h_{o,j} \cdot A_{out} \cdot \frac{(T_{g,out,j} - T_{wall,j}) - (T_{g,in,j} - T_{wall,j})}{\ln\left(\frac{T_{g,out,j} - T_{wall,j}}{T_{g,in,j} - T_{wall,j}} \right)} \right] + \\ & \left[n_j \cdot k_{rad} \cdot S_j \cdot (T_f - T_{wall,j}) \right] \end{aligned} \right) = n_j \cdot \left(\frac{\left(\frac{T_{wall,j} - T_{w,out,j}}{T_{wall,j} - T_{w,in}} \right) - \ln\left(\frac{T_{wall,j} - T_{w,out,j}}{T_{wall,j} - T_{w,in}} \right)}{\frac{\ln(D_{out}/D_{in})}{2 \cdot \pi \cdot k_{SS} \cdot L} + \frac{1}{h_w \cdot A_{in}}} \right) \quad (14)$$

Eq. (14) is represented the heat balance at water tube wall for each considered row ($j = 1, 2, \text{ and } 3$). The heat transfer contributions will be obtained by solving this equation. However, the only unknown in this equation is T_{wall} , which cannot be measured directly from the experiment. Therefore, an exact value of T_{wall} will be obtained by using trial and error technique to guess the value of T_{wall} until Eq. (16) is satisfied. Then, the heat transfer contributions obtained for each row will be summed into the total contributions rate as represent in the Eqs. (3), (4), and (8).

5. Results and discussion

In following section, the experimental results are performed at different equivalence ratio ($\phi = 0.61-0.83$) in order to investigate the performance of the PCH at 21 kW of heat input. The thermal structures in terms of the axial temperature distribution are illustrated in Fig. 3. The major pollutant emissions (CO and NO_x)

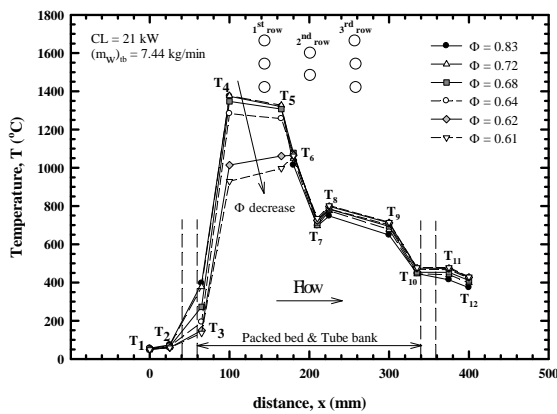


Fig. 3 Effect of ϕ on thermal structures in terms of the axial temperature distribution of the PCH.

levels are addressed to describe the operating range of this present experiment as illustrated in Fig. 4. Moreover, the thermal performance is presented as average heat transfer rate per total surface area ($Q'' = Q/A_{tb}$), whereas Q is calculated from Eqs. (1) - (4) and (8), in order to represent the overall heat transfer performance to the tube bank of PCH as illustrated in Fig. 5.

According to Fig. 3, It clearly seen that maximum combustion temperatures markedly decrease with ϕ , since the thermal input is proportional to it. At particular equivalence ratio, decreasing ϕ may also result in the increasing of gas mixture velocity. If the velocity of gas mixture in the porous medium is higher than the corresponding flame speed, the flame zone can be pushed downstream closer to the tube bank.

This results in the increasing of the experimented heat transfer performance ($Q''_{tb,exp}$) with decreasing ϕ as illustrated in Fig. 5 (within the range of $0.64 < \phi < 0.83$). With flame closer to the tubes ($\phi = 0.64$), a large fraction of heat is extracted by water resulting in the highest $Q''_{tb,exp}$ of 274 kW/m^2 . Furthermore, if ϕ is continuously decreased (less than 0.64), the flame zone,

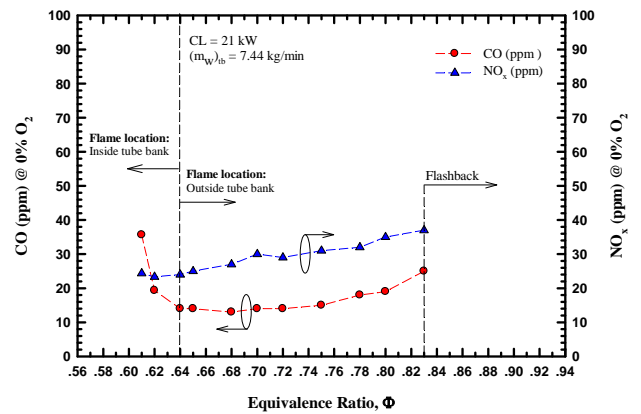


Fig. 4 Effect of ϕ on CO and NO_x emissions of the PCH.

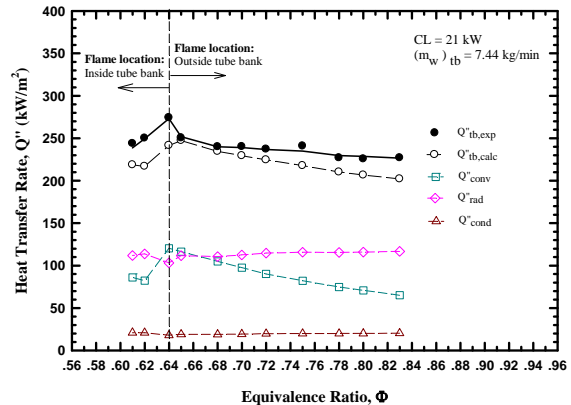


Fig. 5 Effect of ϕ on heat transfer performance and heat transfer contribution of the PCH.

which indicates by the maximum temperature, could also be pushed toward and changed its location from outside (T_4) to locate within the tube bank between first and second row (T_6) as illustrated in Fig. 3. This results in the

dramatically decreased of $Q''_{tb,exp}$ with ϕ as shown in Fig. 5, where ϕ is less than 0.64.

Similar to the thermal structure, equivalence ratio also has a significant influence on combustion emissions as illustrated in Fig. 4. As expect, NO_x emission steadily decreases with decreasing ϕ because of the decreasing in combustion temperature. However, unlike NO_x emission, CO is not significantly affected by the combustion temperature. As flame zone located outside the tube bank ($0.64 < \phi < 0.83$), CO gradually decrease with ϕ . This may be attributed by well mixing quality between air and fuel. In contrast, if the flame zone is continuously pushed in to the tube bank by decreasing ϕ (less than 0.64), CO dramatically increase because of flame quenching. The results also show that within the operating range CO and NO_x emission still not exceeds 40 ppm, which is relatively low.

Furthermore, as shown in Fig. 5, the calculated heat transfer performance ($Q''_{tb,calc}$) shows the same trends with $Q''_{tb,exp}$ but are generally lower, and the discrepancy between those two is about 10% showing that the simplified calculation method reasonably agrees well with the experimental one. Therefore, the calculated heat transfer contributions could be described as the actual heat transfer phenomena occurring in the PCH.

The influence of ϕ on the heat transfer contributions is also illustrated in Fig. 5. As flame located outside tube bank ($0.64 < \phi < 0.83$), convective contribution (Q''_{conv}) is enhanced while ϕ is decreased because gas flow velocity is increased resulting in the thinning of thermal boundary layer around tube surface. In contrast,

the radiative contribution (Q''_{rad}) is slightly decreased with the decreasing in combustion temperature while ϕ is decreased. However, when flame located within the tube bank ($\phi < 0.64$), Q''_{conv} is dramatically decreased because flame is pushed to be located between the first and second row resulted that first row is suddenly cooled by fresh mixture. On the other hand, Q''_{rad} is slightly increased when flame located within the tube bank.

According to Fig. 5, it is clearly seen that both convection and radiation play an important role for transferring combustion heat to the tube bank. Radiative contribution is enhanced when operated at rich condition (up to 58% of the total rate at $\phi = 0.83$), but convective contribution is enhanced when operated at lean condition (up to 50% of the total rate at $\phi = 0.64$). However, conduction, which is not significantly enhanced the heat transfer to the tube bank, contributes only about 10% of the total rate.

6. Conclusion

6.1 This work broadens the knowledge of the PCH by explored its thermal structure and heat transfer contributions to the tube bank.

6.2 The flame zone location show significantly affect on both heat transfer and combustion performance. The highest heat transfer rate of 274kW/m^2 with extremely low CO and NO_x emission (i.e. 14ppm and 24ppm, respectively) is obtained when flame located closer to the tube bank at optimum equivalence ratio of 0.64.

6.3 Both convection (i.e. enhanced up to 50% of the total rate at lean condition) and radiation (i.e. enhanced up to 58% of the total rate at rich



condition) are the significant contribution to transfer combustion heat to the tube bank.

7. Recommendation for future work

In order to enhance the heat transfer performance, the PCH will be equipped with Cyclic Flow Reversal Combustion (CFRC) technique [4], which will be the topic for further investigation.

8. Acknowledgments

This study was sponsored by the Ministry of Education, Royal Thai Government under the project of Thailand National Research Universities (NRU).

9. References

- [1] Howell, J.R., Hall, M.J. and Ellzey, J.L. (1996). Combustion of Hydrocarbon Fuels within Porous Inert Media, *Progress in Energy and Combustion Science*, Vol. 22(2), February 1999, pp. 121-145.
- [2] Xiong, T.Y., Khinkis, M.J. and Fish, F.F. (1995). Experimental study of a high efficiency, low emission porous matrix combustor-heater, *Fuel*, Vol. 74(11), November 1995, pp. 1641-1647.
- [3] Jun-Rui Shi, Mao-Zhao Xie, Hong Lui, Hong-Sheng Liu, Xue-Song Zhang and You-Ning Xu (2010). Two-dimensional numerical study of combustion and heat transfer in porous media combustor-heater, *Proceeding of Combustion Institute*, Vol. 33(2), October 2010, pp. 3309-3316.
- [4] Jugjai, S. and Nungniyom V. (2009). Cyclic operation of porous combustor-heater (PCH), *Fuel*, Vol. 88(3), March 2009, pp. 553-559.

[5] Incropera, F.P. and DeWitt, D.P. (2001). *Fundamental of Heat and Mass Transfer*, Wiley, New Jersey.

[6] Nasr, K. (1993). *Experimental and Numerical Studies of Forced Convection and Radiation Heat Transfer in Packed Beds*, Ph.D. Thesis in Mechanical Engineering of Purdue University, Indiana.

[7] Mohammad, L. (2008). Numerical Analysis of Wooden Porous Media Effects on Heat Transfer from Staggered Tube Bundle, *Journal of Heat transfer*, Vol. 130(1), pp. 014501-1 - 014501-6.